

Improving stability domains of the implicit higher order accuracy method

M. Rezaiee-Pajand^{*,†,‡}, S. R. Sarafrazi and M. Hashemian

Department of Civil Engineering, Ferdowsi University of Mashhad, Mashhad, Iran

SUMMARY

The implicit higher order accuracy (IHOA) time integration family has a high order of accuracy. However, its stability domains are very restrictive. By improving the stability conditions, the larger time steps can be utilized. In this study, two parameters are introduced in the displacement and velocity extrapolations of IHOA. In order to find the optimum values of the proposed parameters, the dissipation and the dispersion are investigated. Three conditionally stable versions of the second-, third-, and forth-order algorithms are found. It is shown that these formulations have larger stability domains than the previous ones. Furthermore, the suggested strategies give responses that are more accurate. Copyright © 2011 John Wiley & Sons, Ltd.

Received 6 January 2011; Revised 1 March 2011; Accepted 6 March 2011

KEY WORDS: nonlinear dynamic analysis; numerical time integration; implicit higher order accuracy process; improving stability

1. INTRODUCTION

Direct time integration techniques have been powerful tools for solving the differential equation of motion for decays. Numerical algorithms divide the time domain in finite and small enough time steps. Then, the system solution is found step-by-step. Some assumed functions are utilized in establishing the required formulations. Using the approximated functions leads to three types of errors in the obtained responses, which are dissipation, dispersion, and overshooting [1]. Dissipation refers to the presence of numerical amplitude decay or numerical damping. Moreover, the dispersion results in shortening or elongating the natural period of vibration. Finally, overestimating the exact solution in the first few steps of the algorithm is called overshooting. As a reminder, the responses are usually damped after proceeding noticeable steps. If amplitude errors grow irrepressibly, the results will diverge from the exact solution and the procedures will be unstable.

All time integration schemes can be classified as explicit, implicit, and predictor-corrector ones [2]. The implicit interpolation functions are written in terms of unknown responses at the end of time steps. Consequently, an iterative procedure should be employed to analyze the nonlinear systems. On the other hand, the explicit tactics use the known variable in their extrapolations. Furthermore, the latter system of equations is written in terms of accelerations. In other words, the coefficient matrix is the mass matrix. Solving the mentioned system of equations is very simpler than the implicit one. However, the outcomes of explicit methods have no acceptable accuracy in nonlinear problems. Researchers merge the abilities of the explicit and implicit algorithms and

*Correspondence to: M. Rezaiee-Pajand, Department of Civil Engineering, Ferdowsi University of Mashhad, Mashhad, Iran.

[†]E-mail: mrpajand@yahoo.com

[‡]Professor.

present the predictor-corrector techniques. These processes obtain an approximate solution using an explicit strategy and correct them utilizing an implicit method.

Newmark presented the most popular implicit method in 1959 [3]. The simplicity and the second-order accuracy make it a famous and effective scheme. As a result, this procedure has been employed for the dynamic analysis of many practical engineering structures, during the past 50 years. The Newmark approach relies on the direct use of Taylor's series by employing the two well-known parameters, β and γ , that define the accuracy and stability properties of the numerical integration method. Setting $\beta=1/4$ and $\gamma=1/2$ results in Newmark average acceleration (NAA) technique, which is unconditionally stable. The obtained process utilizing $\beta=1/6$ and $\gamma=1/2$ is not always stable but models the linear acceleration functions accurately [3]. Since 1959, many studies have been done to improve the Newmark method. In 1973, Wilson *et al.* proposed the famous implicit Wilson- θ technique, in which the parameter θ was used to obtain an unconditionally stable time integration process [4]. Some other investigations, such as the WBZ- α [5], HHT- α [6], and generalized- α [7], introduced extra parameters to impose artificial damping on the responses and control the stability and the higher order dissipation.

It is worth emphasizing that most second-order time integration algorithms use only the last available solutions to extrapolate the system responses at the end of time step. To improve the accuracy of answers, one can employ the information of previous time steps. This action can be done by taking advantage of the higher order interpolation. Zhai utilized this idea and offered a second-order explicit and predictor-corrector algorithms, which use the accelerations of two previous time steps [8]. Rezaiee-Pajand and Alamatian extended Zhai formulation and proposed a higher order predictor-corrector family, in which the displacement and velocity interpolations invoke the accelerations at several earlier time points [9]. They also suggested an implicit higher order accuracy (IHOA) time integration family in a parallel manner [10]. In 2005, Keierleber and Rosson utilized a similar technique to propose an implicit algorithm [11]. They assumed the acceleration as a higher order polynomial over each time step interval. By using a θ parameter, like the Wilson- θ method, they improved the accuracy and stability of their proposed process, as well.

The IHOA time integration family utilizes some weighted factors to control the accuracy of the numerical integration and permits the time step to control the stability of the algorithm [10]. Although this family presents high-accuracy results in solving various types of linear and nonlinear structural problems, its stability conditions are very cumbersome. Based on this fact, increasing the stability limits of some members of the IHOA family is pursued in this paper. At first, the fundamental equations and characteristics of the IHOA method are presented. Then, an idea for improving the current IHOA procedure is introduced, and the way of attaining the essential parameters for improving each member of the IHOA family is described. After that, the stability conditions of the suggested IHOA procedures are compared with the previous ones. Finally, some linear and nonlinear problems are solved to numerically validate the new properties of the proposed formulations. Due to volume limitation of the article, only some parts of the numerical experiences are presented here.

2. THE IHOA METHOD

The linear and nonlinear dynamic equilibrium equations of motion and its initial conditions are written in the following form [12]:

$$\mathbf{M}\ddot{\mathbf{X}} + \mathbf{C}\dot{\mathbf{X}} + \mathbf{K}\mathbf{X} = \mathbf{P} \quad (1)$$

$$\mathbf{X}(0) = \mathbf{X}_0, \quad \dot{\mathbf{X}}(0) = \dot{\mathbf{X}}_0 \quad (2)$$

where \mathbf{K} , \mathbf{C} , and \mathbf{M} are stiffness, damping, and mass matrices, correspondingly, and \mathbf{P} shows the vector of external forces. The nodal displacement vector and its derivatives are also denoted by: \mathbf{X} , $\dot{\mathbf{X}}$, and $\ddot{\mathbf{X}}$, respectively. The main goal is finding the system responses by satisfying Equation (1) at the finite points of the time domain. This target can be achieved by utilizing a proper numerical time integration algorithm. Recently, Rezaiee-Pajand and Alamatian suggested an IHOA time

Table I. Values of ζ and η for the IHOA method.

m	ζ_{mj}				η_{mj}			
	$j=0$	$j=1$	$j=2$	$j=3$	$j=0$	$j=1$	$j=2$	$j=3$
2	0.12500000	-0.04166667	—	—	0.41666667	-0.08333333	—	—
3	0.10555556	-0.10000000	0.01944444	—	0.37500000	-0.20833333	0.04166667	—
4	0.09375000	-0.17083333	0.06666667	-0.01180556	0.34861111	-0.36666667	0.14722222	-0.02638889

Table II. The stability limits for IHOA-2, 3, and 4.

Accuracy order	$\Delta t / T$
2	Unstable
3	Unstable
4	0.18

integration family and denoted it as IHOA- m [10]. The parameter m shows the accuracy order of this method. The displacement and velocity relations for the IHOA- m family are given below:

$$\mathbf{X}_{i+1} = \mathbf{X}_i + \Delta t \dot{\mathbf{X}}_i + \left(\frac{1}{2} - \sum_{j=0}^{m-1} \zeta_{mj} \right) \Delta t^2 \ddot{\mathbf{X}}_i + \zeta_{m0} \Delta t^2 \ddot{\mathbf{X}}_{i+1} + \Delta t^2 \sum_{j=1}^{m-1} \zeta_{mj} \ddot{\mathbf{X}}_{i-j} \tag{3}$$

$$\dot{\mathbf{X}}_{i+1} = \dot{\mathbf{X}}_i + \left(1 - \sum_{j=0}^{m-1} \eta_{mj} \right) \Delta t \ddot{\mathbf{X}}_i + (\eta_{m0}) \Delta t \ddot{\mathbf{X}}_{i+1} + \Delta t \left(\sum_{j=1}^{m-1} [(\eta_{mj}) \ddot{\mathbf{X}}_{i-j}] \right) \tag{4}$$

In these equations, \mathbf{X}_{i+1} and $\dot{\mathbf{X}}_{i+1}$ are unknown displacement and velocity vectors at time t_{i+1} , respectively. The acceleration vector at time $t_i - j \Delta t$ is denoted by $\ddot{\mathbf{X}}_{i-j}$ and should be kept in computer memory. The weighted factors, ζ_{mj} and η_{mj} , are calculated in such a way that each member has the complete order. The aforementioned parameters for the second-, third-, and fourth-order members of IHOA are arranged in Table I [10].

The weighted factors affect the stability properties of the IHOA family. Indeed, these methods are not unconditionally stable. The stability conditions of the mentioned members of the IHOA family are presented in Table II. It shows that the second- and third orders of this family are mathematically unstable. However, their spectral radius for very fine time steps is close to 1 and they act like a stable process. Moreover, the stability limit of IHOA-4 is approximately 33% of the stability limit of linear acceleration method of Newmark. In other words, the stability conditions of the IHOA family are very restrictive. Because of higher order accuracy, it is desirable to improve the stability limit of IHOA. The next section shows the process of achieving this target.

3. STABLE IHOA FAMILY

Increasing the stability limits of the IHOA time integration family is the object of this section. For this purpose, two variables like β and γ in the Newmark method are introduced in the IHOA extrapolations. These parameters enable the analyst to increase the stability domain and minimize the truncation error. Based on this idea, β_m and γ_m factors are added to the last terms of Taylor’s series for displacement and velocity, respectively. In other words, the below extrapolations are employed:

$$\mathbf{X}_{i+1} = \sum_{j=0}^{m+1} \left(\frac{\Delta t^j}{j!} \ddot{\mathbf{X}}_i \right) + \Delta t^{m+2} \left(\frac{1}{(m+2)!} + \beta_m \right) \ddot{\mathbf{X}}_i \tag{5}$$

$$\dot{\mathbf{X}}_{i+1} = \sum_{j=0}^m \left(\frac{\Delta t^j}{j!} \dot{\ddot{\mathbf{X}}}_i \right) + \Delta t^{m+1} \left(\frac{1}{(m+1)!} + \gamma_m \right) \dot{\ddot{\mathbf{X}}}_i \tag{6}$$

Table III. Values of c coefficients.

$c_{mj}, j = 1, 2, 3$			
m	1	2	3
2	1		
3	3	-1	
4	6	-4	1

In these relations \mathbf{X}_i^j is the j th derivative of the displacement vector at time t_i . Rezaiee-Pajand and Alamatian used the backward Taylor’s series to obtain the accelerations of the previous steps in the terms of the higher order derivatives [10]. By utilizing their relations, Equations (5) and (6) can be rewritten in the following form:

$$\begin{aligned} \mathbf{X}_{i+1} = \mathbf{X}_i + \Delta t \dot{\mathbf{X}}_i + \left(\frac{1}{2} - \sum_{j=0}^{m-1} \xi_{mj} - m\beta_m \right) \Delta t^2 \ddot{\mathbf{X}}_i + (\xi_{m0} + \beta_m) \Delta t^2 \ddot{\mathbf{X}}_{i+1} \\ + \Delta t^2 \left(\sum_{j=1}^{m-1} [(\xi_{mj} + c_{mj} \beta_m) \ddot{\mathbf{X}}_{i-j}] \right) \end{aligned} \tag{7}$$

$$\begin{aligned} \dot{\mathbf{X}}_{i+1} = \dot{\mathbf{X}}_i + \left(1 - \sum_{j=0}^{m-1} \eta_{mj} - m\gamma_m \right) \Delta t \ddot{\mathbf{X}}_i + (\eta_{m0} + \gamma_m) \Delta t \ddot{\mathbf{X}}_{i+1} \\ + \Delta t \left(\sum_{j=1}^{m-1} [(\eta_{mj} + c_{mj} \gamma_m) \ddot{\mathbf{X}}_{i-j}] \right) \end{aligned} \tag{8}$$

It should be noted that c_{mj} coefficients are constant and their values are according to Table III. One can change the order m and find the members of the IHOA family. This group of the numerical time integration algorithms is called MIHOA. Three members of this family with $m = 2, 3,$ and 4 are selected for more studies. In order to perform stability and accuracy analyses, the optimum values of β_m and γ_m are calculated in the next section. It should be added that the unconditional stable MIHOA-2 is similar to the one which was proposed by Karimie-Rad and Ghassemieh [13]. It is worthwhile to know that they utilized a different way of applying the parameters β_2 and γ_2 to the main equations. In fact, the conditional stable MIHOA-2, MIHOA-3, and MIHOA-4 tactics are new.

4. THE OPTIMUM VALUES OF β_m AND γ_m

If the analyst transforms the system of dynamic equilibrium equations into modal space, Equation (1) can be converted to n uncoupled relations. These independent equations are similar and can be written in the below general form:

$$\ddot{x} + 2\zeta\omega\dot{x} + \omega^2x = r \tag{9}$$

In other words, a structure with several degrees of freedom (MDOF) can be converted to a single degree of freedom (SDOF) system with angular frequency ω , damping ratio ζ , and external load r . Consequently, it is sufficient to study the stability of these SDOF systems instead of MDOF. On the other hand, as the stability property of a numerical time integration method is independent of initial conditions, the external load is assumed to be zero [12]. Furthermore, it is usual to study the stability of a numerical tactic on an un-damped system. The analysts’ experiences show that the results of the aforementioned way of investigation can be extended to the complex and

large systems [14, 15]. As a result, the succeeding equilibrium equation for a free oscillation and undamped SDOF structure is considered:

$$\ddot{x} + \omega^2 x = 0 \quad (10)$$

A numerical time integration procedure is an iterative method. Since the applied external load is zero, the unknown variables at time t_{i+1} for a linear problem can be related to the displacement, velocity, and acceleration at time t_i in the following form:

$$\begin{Bmatrix} \ddot{x}_{i+1} \\ \dot{x}_{i+1} \\ x_{i+1} \end{Bmatrix} = \mathbf{A} \times \begin{Bmatrix} \ddot{x}_i \\ \dot{x}_i \\ x_i \end{Bmatrix} \quad (11)$$

In the last equation, \mathbf{A} is the amplification matrix, which is depended on the augular frequency, time step, and the interpolation coefficients. The IHOA and MIHOA use the acceleration of several previous time steps. As a result, the amplification matrix is a rectangular matrix and the order of its characteristic polynomial is more than 3. In order to obtain a square amplification matrix, some relations like $\ddot{x}_j = \ddot{x}_i$ ($j = i, i-1, \dots, i-m+2$) are added to the system of equations (11). Accordingly, the below iterative relation is on hand:

$$\begin{Bmatrix} \ddot{x}_{i+1} \\ \vdots \\ \ddot{x}_{i-m+2} \\ \dot{x}_{i+1} \\ x_{i+1} \end{Bmatrix} = \mathbf{A} \times \begin{Bmatrix} \ddot{x}_i \\ \vdots \\ \ddot{x}_{i-m+1} \\ \dot{x}_i \\ x_i \end{Bmatrix} \quad (12)$$

The iterative process of Equation (12) is stable when the responses do not grow up irregularly. On the other hand, the procedure is also stable if the amplification matrix is remained bounded. This target can be achieved by restricting the eigenvalues of \mathbf{A} . It is reminded that the highest absolute eigenvalue is denoted by ρ , which is the spectral radius of \mathbf{A} . The numerical time integration will be stable, if the relation $\rho = \max(\lambda_j) \leq 1$ is held. It is clear that the value of the spectral radius depends on the values of ω and Δt . In structural dynamics, ρ is presented via the ratio of $\Delta t/T$, where $T = 2\pi/\omega$ is the period of the system. The numerical method is unconditionally stable when the value of spectral radius does not exceed 1 for all $\Omega = \Delta t/T \in [0, \infty)$ [7]. If the inequality equation $\rho \leq 1$ is satisfied for a certain $\Delta t/T$ domain, the algorithm is conditionally stable. Based on these properties, the stability of the MIHOA family is investigated. To find the spectral radius, the characteristic polynomial of the suggested time integration family is presented in the formula below:

$$\begin{aligned} & [1 + (\zeta_{m0} + \beta_m)\Omega^2]\lambda^{m+1} + \left[\left(\frac{1}{2} + \eta_{m0} - 2\zeta_{m0} - \sum_{j=1}^{m-1} \zeta_{mj} - (m+1)\beta_m + \gamma_m \right) \Omega^2 - 2 \right] \lambda^m \\ & + \left[\left(\frac{1}{2} + \zeta_{m1} - \sum_{j=0}^{m-1} (\eta_{mj} - \zeta_{mj}) + \frac{1}{2}m(m+1)\beta_m - m\gamma_m \right) \Omega^2 + 1 \right] \lambda^{m-1} \\ & + \Omega^2 \sum_{j=1}^{m-2} [(\eta_{mj} - \zeta_{mj} + \zeta_{m(j+1)}) + (-c_{mj} + c_{m(j+1)})\beta_m + c_{mj}\gamma_m] \lambda^{m-j-1} \\ & + \Omega^2 (\eta_{m(m-1)} - \zeta_{m(m-1)} + (-1)^m (\gamma_m - \beta_m)) = 0 \end{aligned} \quad (13)$$

At first stage, the IHOA-2 tactic is studied. After substituting the order m in Equation (13) by 2 and solving it, the spectral radius can be found. Satisfying $\rho \leq 1$ when Ω goes to infinity leads to

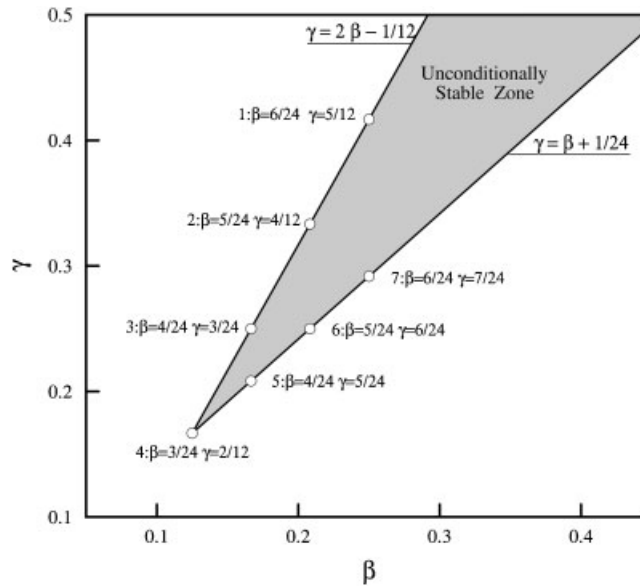


Figure 1. The unconditionally stable zone for different values of β_2 and γ_2 .

the below conditions:

$$\beta_2 + \frac{1}{24} \leq \gamma_2 \leq 2\beta_2 - \frac{1}{12} \tag{14}$$

$$\gamma_2 \geq \frac{1}{6} \tag{15}$$

Equations (14) and (15) are plotted in Figure 1. This figure shows the stable zone for IHOA-2. It is important to note that using each point in the stable zone or on its boundaries produces an unconditionally stable algorithm. From this point forward the developed method will be called MIHOA-2U.

A comprehensive study has been done among the infinite stable cases of the IHOA-2 tactics, which have the minimum value of error. Some specific points are shown in Figure 1, which are used to find optimum values of β_2 and γ_2 . For this purpose, the values of dissipation and dispersion for the MIHOA-2U procedure are calculated when different values of β_2 and γ_2 are utilized. Some sample time steps have been chosen for error analysis. The amplitude decay is equal to zero for all points specified in Figure 1. Figure 2 shows the period elongation (PE) for these points. Based on this figure, it can be seen that the optimum values of β_2 and γ_2 are 1/8 and 1/6, correspondingly, which belong to point 4.

It is worth emphasizing that the lower limit of Equation (14), $\gamma_2 = \beta_2 + 1/24$, specifies an interesting limit for stability of the method in practical time steps. Therefore, some points on this limit are selected and the period and the amplitude errors are also calculated. Since all the amplitude errors are very close to zero, just the PE errors are compared in Figure 3. It should be noted that the relation $\gamma_2 \leq 1/6$ is held and the condition $\gamma_2 \leq 2\beta_2 - 1/12$ is ignored. Consequently, not all selected points present unconditionally stable techniques.

As it can be seen in Figure 3, point 5 with $\beta_2 = -1/24$ and $\gamma_2 = 0$ has the minimum PE. This value is even less than that belongs to point 1 with $\beta_2 = 1/8$ and $\gamma_2 = 1/6$, which is related to the optimum point for unconditional stability. It is easy to show that applying the values of $\beta_2 = -1/24$ and $\gamma_2 = 0$ leads to conditionally stable version of the IHOA-2 scheme. This version is denoted as MIHOA-2C

In the following, the stability of MIHOA-3 strategy is investigated. It should be noted that the analytical solution of the characteristic polynomial for the MIHOA-3 technique is very complicated. In fact, the optimum values for β_3 and γ_3 can be found numerically. In order to reach this goal,

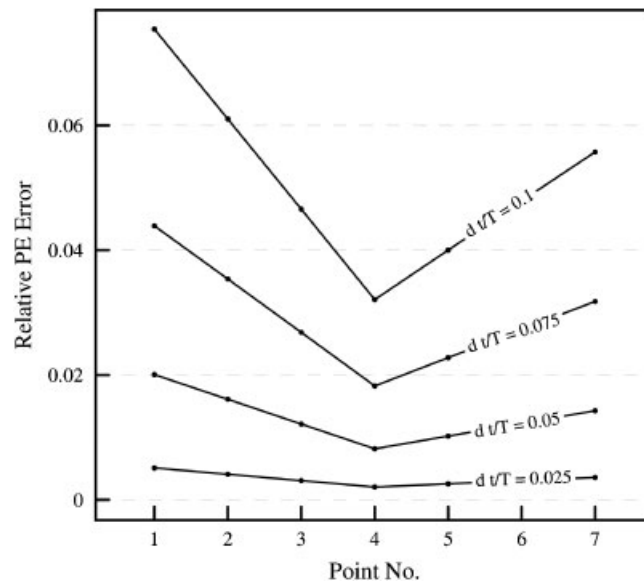


Figure 2. Relative PE error of IHOA-2 for some points of the unconditionally stable zone.

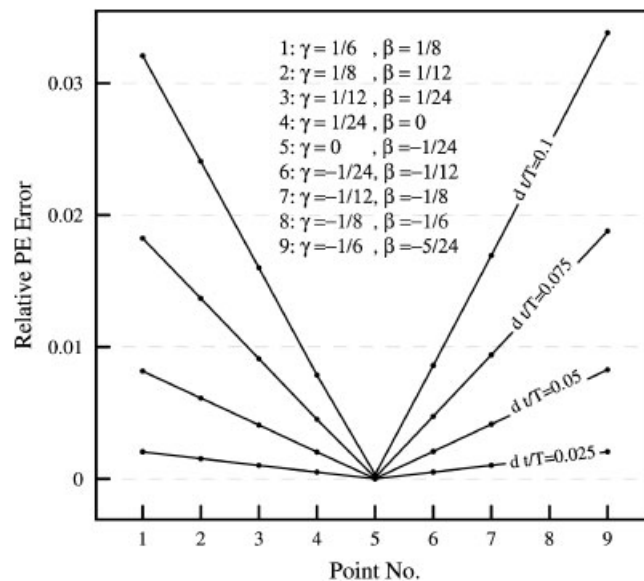


Figure 3. Relative PE error for some points of line $\gamma_2 = \beta_2 + 1/24$ with $\gamma_2 \leq 1/6$.

a wide range of β and γ pairs and different values of $\Delta t/T$ ratios are selected. Utilizing these values, the stability spaces are searched. Figure 4 shows the boundaries of the stability zones. These areas are bounded by β axis, γ axis, and curved lines for different values of time steps. It is worthwhile to add that the curved lines are the locus of (β_3, γ_3) points that produce the methods with spectral radius equal to 1. As it is shown in Figure 4, all the curved lines pass through the point $(-1/45, 0)$. Consequently, it is sensible to take $\beta_3 = -1/45$ and $\gamma_3 = 0$ for the MIHOA-3 process. It is important to note, when the time step is approximately greater than $0.38T$, there is no stability space. In other words, MIHOA-3 is conditionally stable.

In a similar way, the optimum values of β_4 and γ_4 are obtained for the MIHOA-4 algorithm. Figure 5 shows the boundaries of the stability zones for some values of the $\Delta t/T$ ratio, when

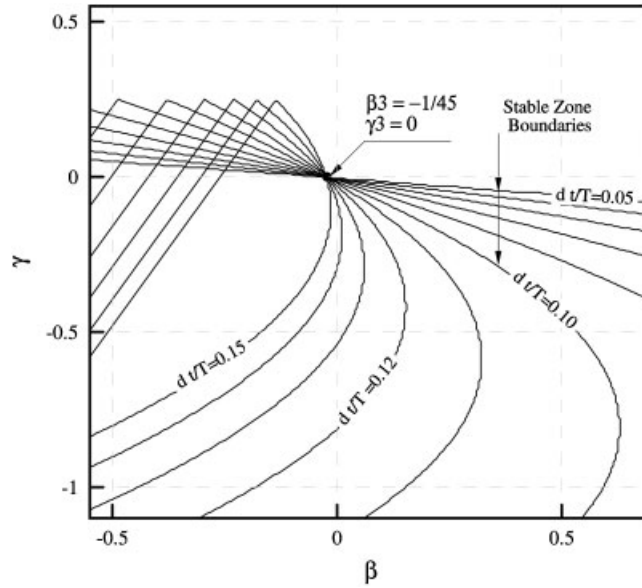


Figure 4. Stable zones of MIHOA-3 for different time steps in the $\beta-\gamma$ space.

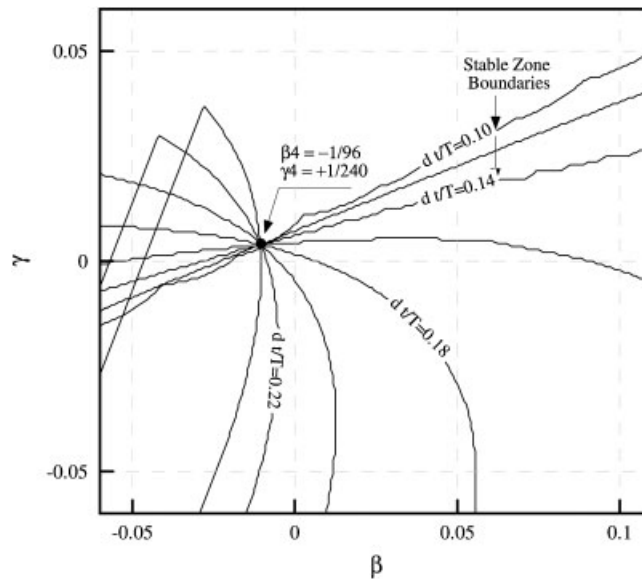


Figure 5. Stable zones of MIHOA-4 for different time steps in the $\beta-\gamma$ space.

the MIHOA-4 procedure is utilized. The point $(-1/96, 1/240)$ is also common for all aforementioned curves. Consequently, the MIHOA-4 method is constructed using $-1/96$ and $1/240$ for β_4 and γ_4 , respectively. It is easy to realize, when the time step is greater than $0.38T$, there is no (β_4, γ_4) point to stabilize the MIHOA-4 tactic. In this case, the proposed scheme is conditionally stable.

Following the aforementioned discussion, a summary of the optimum parameters and stability limits for the suggested higher order implicit time integration strategies is presented in Table IV. The curves of spectral radius for the proposed formulation, the IHOA-2, 3, and 4 tactics are plotted in Figure 6.

Table IV. Parameters and stability limits for the MIHOA family.

m	β_m	γ_m	Type of stability	Stability limit
2	1/8	1/6	US	∞
2	-1/24	0	CS	0.38
3	-1/45	0	CS	0.38
4	-1/96	1/240	CS	0.38

US: unconditional stability; CS: conditional stability.

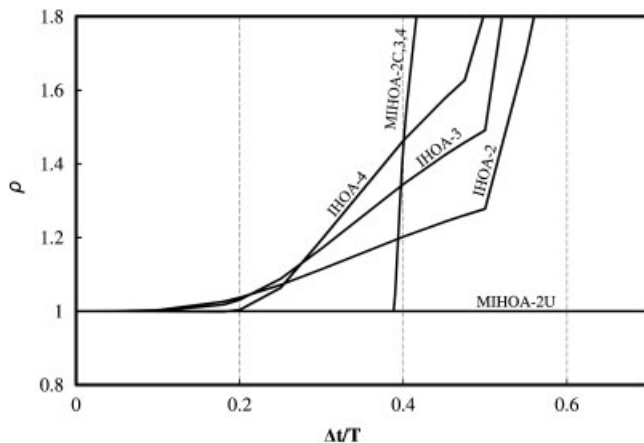


Figure 6. The spectral radius curves.

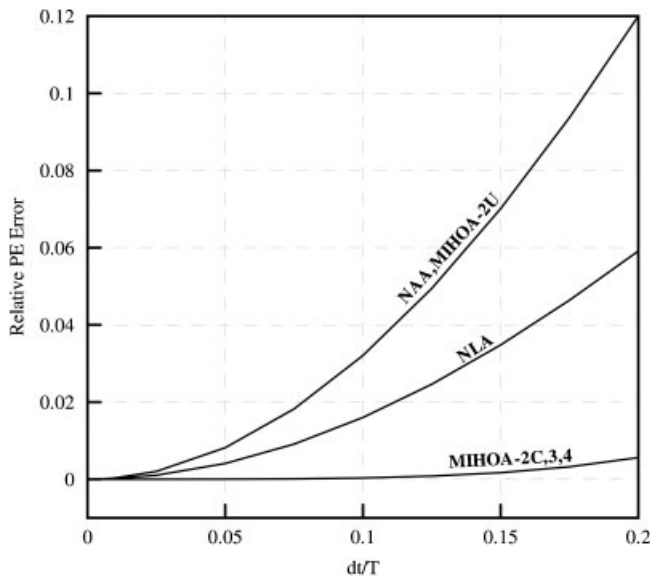


Figure 7. Relative PE error for the proposed and Newmark methods.

The value of the spectral radius of the MIHOA-2U method is equal to 1 for all $\Delta t/T \in [0, \infty)$. An interesting point is that the spectral radius curves are the same for all conditional suggested schemes, which are called MIHOA-2C, 3, and 4. Moreover, the calculated limit for all of these conditional stable approaches equals to 0.38.

In order to compare the accuracy of the proposed techniques with the NAA scheme and the Newmark linear acceleration (NLA) method, PE of all these procedures is illustrated in Figure 7.

Based on this fact that the amplitude decays of all approaches are equal or very close to zero, the differences between the amplitude values are not noticeable. Figure 7 shows that NAA and MIHOA-2U have same PE. It is important to note that the accuracy of proposed conditionally stable algorithms is much better than both the Newmark procedures. Another fact is that, since the behaviors of the spectral radius of all suggested conditionally stable strategies are very similar to each other, their PEs are identical.

5. NUMERICAL EXAMPLES

In this section, a variety of examples are solved using both linear and nonlinear analysis. To substantiate the advantages of the proposed formulations against the available methodologies, the results of all algorithms are compared with the exact or quasi-exact solutions. It should be noted that the quasi-exact solution is found by employing a very miniature time step and performing the NAA procedure. According to [12], the NAA scheme is the most common technique for both linear and nonlinear dynamic analysis among the other implicit approaches. In order to select a proper time step for attaining the near exact solution, the outcomes of using Δt are compared with those obtained by employing $0.5\Delta t$. If the two sets of results have no sizeable difference, a suitable time step is on hand. In all of the presented examples, the Newmark average acceleration, the Newmark linear acceleration, and the Wilson- θ process are called NAA, NLA, and WTM, respectively.

5.1. Cantilever plane truss

Gu *et al.* studied a structural model of a cantilever plane truss, with 25 similar bays [16]. This structure is shown in Figure 8. The Young's modulus and density of the truss are 210 GPa and 7850kg/m^3 , respectively. Each bar has an area section equal to $1.96 \times 10^{-3}\text{m}^2$.

The aforementioned structure is excited by an initial vertical displacement at the node D. Utilizing the proposed time integration strategies, the free vibration response of the system is obtained. According to the Paz model [17], the consistent mass matrix of the system is formed. In order to model elastic geometrically nonlinear behavior of structure, total lagrangian finite element formulation is utilized [9, 10]. The quasi-exact vertical displacement of the node D for free vibration of the system is plotted in Figure 9. As it is shown in the mentioned figure, there is a rapid change in the structural response. Therefore, the capability of the higher order methods is appeared. The time between 0.099 and 0.1 s is selected for comparing the solution of different time integration algorithms in Figure 10. In this example, the time step of 0.0001 s is utilized. It is clear that the IHOA-2 algorithm results in unstable solution, and IHOA-3 and also IHOA-4 tactics do not lead to satisfactory outcomes. Moreover, the WTM curve damps down. However, the MIHOA-2U and NAA are stable but their solutions have considerable errors. On the other hand, the conditionally stable MIHOA formulations can present much better solutions in this nonlinear problem. It is visible that even in nonlinear behavior, the MIHOA-2C approach can reach near exact solutions and therefore it is reasonable to use this second-order tactic than the third- or fourth-order ones.

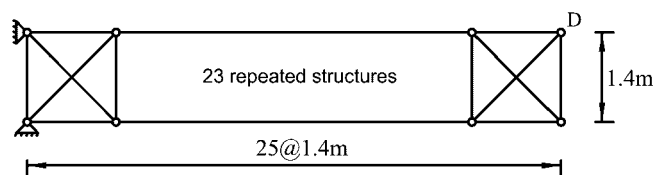


Figure 8. Cantilever plane truss.

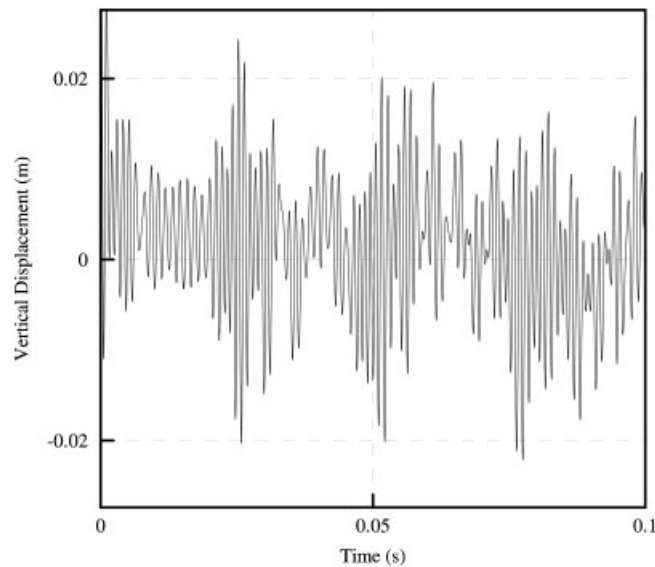


Figure 9. Quasi-exact vibration of cantilever plane truss.

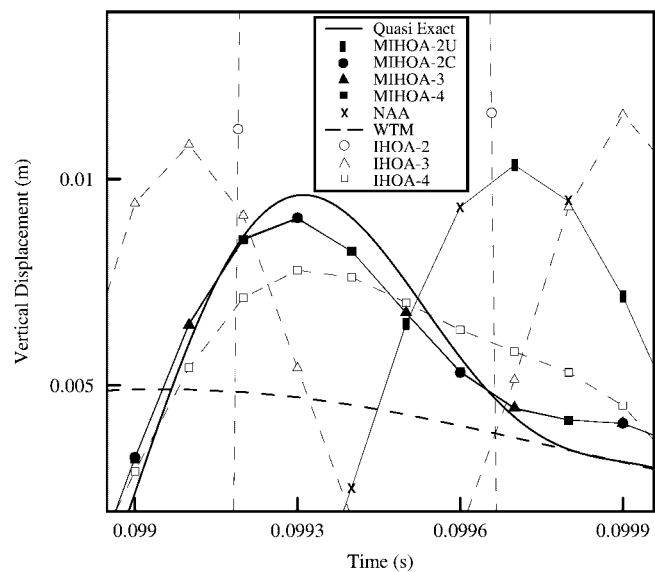


Figure 10. The vertical displacement of point D of cantilever plane truss between 0.099 and 0.1 s.

5.2. Van Der Pol equation

As another example, the second-order differential equation of Van Der Pol oscillator with nonlinear damping is studied. The mentioned dynamic system and its initial conditions are as below:

$$\ddot{D} - 0.1(1 - D^2)\dot{D} + D = 0, \quad D(0) = 2, \quad \dot{D}(0) = 0$$

The exact solution of the given equation has been presented by Anvoner [18], and is plotted for a time interval between 269 to 275 s in Figure 11. To specify the power and ability of the proposed schemes in solving nonlinear dynamic equations, compared with the previous IHOA and also some popular methods, such as WTM and NLA, the solutions of all these algorithms are also displayed in Figure 11.

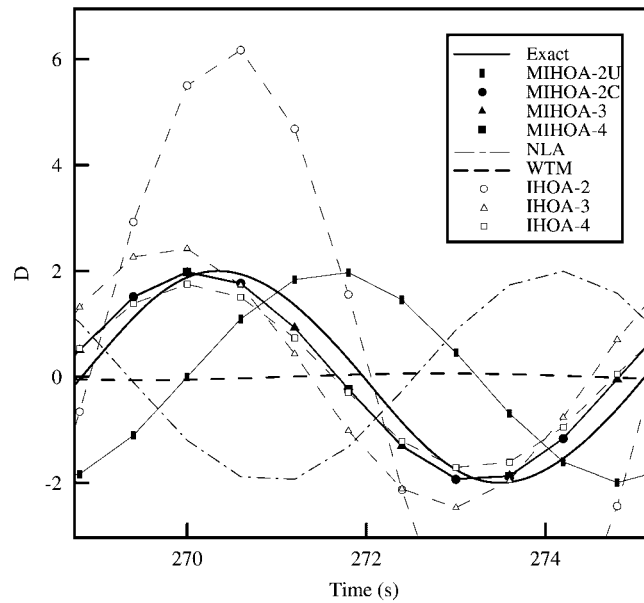


Figure 11. Displacement–time curve for Van Der Pol equation between 269 and 275 s.

As the approximate period of the system is 6.287 s, the time step is considered to be equal to 0.6 s. According to the last figure, NLA and MIHOA-2U have acceptable amplitudes, although they show large PE errors. The IHOA-2 and IHOA-3 processes are unstable and both of them have amplitude error. These procedures have period error as well. However, the error of the IHOA-2 tactic is more than the IHOA-3 one. As it is expected, the IHOA-4 scheme is stable and has better answers than the IHOA-2 and 3 techniques, but clearly the first one damps down the solution. Based on the results of Figure 11, the worst solution belongs to WTM, because of existing numerical damping. Comparing the results of the presented algorithms with the exact solution reveals the power of the suggested formulations for solving the nonlinear problems. The dissipation and dispersion errors of the proposed conditionally stable methods are much less than the other aforementioned techniques. Besides all of these, the stability ranges of these algorithms are wide enough for applying in practical problems. Once again, due to the similarity of the results of these three methods, using the second-order one is more sensible.

5.3. 2D frame

A ten story, 2D steel frame, which was analyzed by Sekulovic *et al.* [19] is considered. In this linear dynamic analysis, the proposed time integration formulations are compared with the other techniques. Figure 12 shows the mentioned frame. The weight and the mass of members are assumed zero. However, the lumped masses are introduced into the nodal points instead. The values of nodal masses, m and m_r , are 8000 and 6000 kg, respectively. The modulus of elasticity is 210 GPa and the section properties of the structural elements are given in Table V. It should be noted that there are no external forces acting on the frame. Indeed, the structure is excited by a ground acceleration as follows:

$$\ddot{x}_g = \begin{cases} 0.2 \text{ m/s}^2 & 0 \leq t \leq 1 \text{ s} \\ 0.4 \text{ m/s}^2 & 1 \text{ s} \leq t \leq 3 \text{ s} \\ 0 & 3 \text{ s} \leq t \end{cases}$$

The maximum horizontal displacement of the frame is pursued under the base excitation. For this purpose, the suggested numerical time integration approaches are selected. The time step is 0.001 s

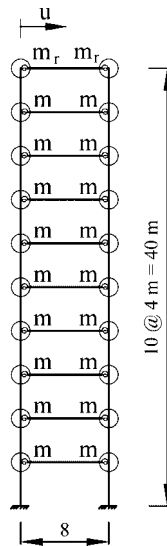


Figure 12. 2D frame.

Table V. The section properties of 2D frame.

Section	Member	Stories	A (m ²)	I (m ⁴)
C1	Column	1-4	0.027	1.71×10^{-3}
C2	Column	5-7	0.0218	7.989×10^{-4}
C3	Column	8-10	0.0149	2.517×10^{-4}
B	Beam	All	0.306	2.569×10^{-3}

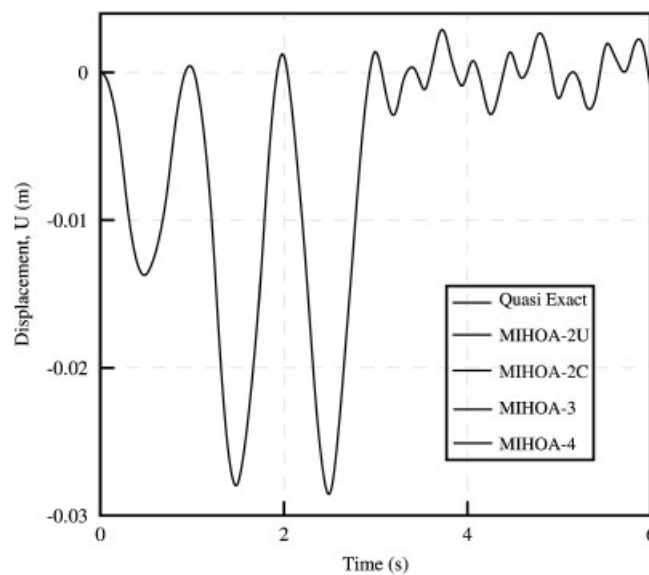


Figure 13. The maximum horizontal displacement of 2D frame, for time step 0.001 s.

for this set of analyses. Figure 13 displays the curve of the index displacement versus time. It is important to note that all the proposed schemes almost coincide with the near exact solution while all the three ordinary higher order tactics, IHOA-2, 3 and 4, are unstable.

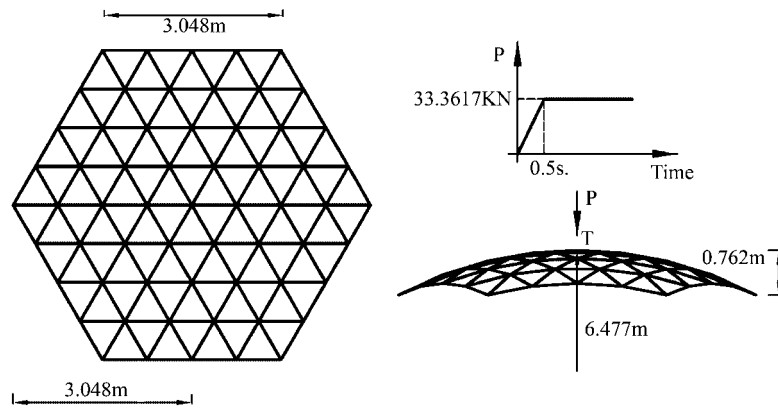


Figure 14. Dome shape truss.

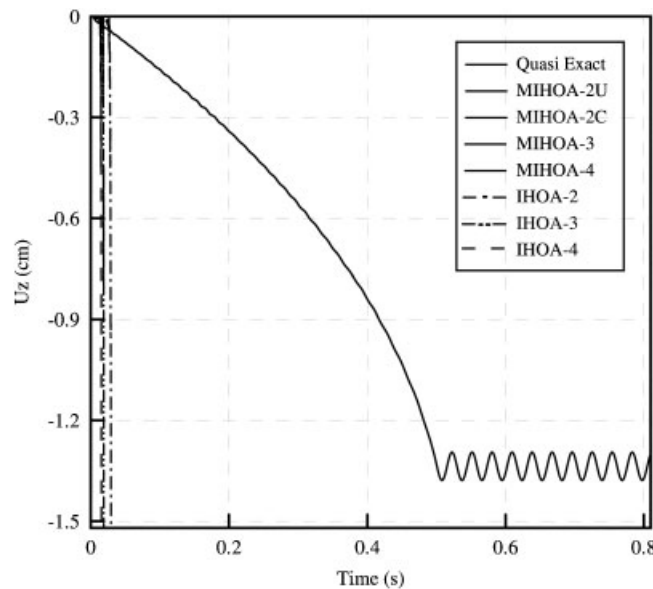


Figure 15. The vertical displacement of point *T* of dome shape truss, for time step 0.0002 s.

5.4. Dome shape truss

Figure 14 shows a 3D dome shape truss with fixed base joints, 156 elements and 111 DOFs. The value of section area for all members is 1290.32mm². The modulus of elasticity and density of the material are 210 GPa and 8303 kg/m³, respectively. A concentrated load is applied on the point *T* on the summit of the dome as shown in Figure 14. The weight of the structure is ignored in this analysis.

Using the ordinary and new IHOA schemes some nonlinear dynamic analyses are performed. In this example the numerical time integration procedures utilize 0.0002 s for time step. Figure 15 shows the results of the vertical displacement at the point *T*. It is clear from the figure that the IHOA-2, 3, and 4 tactics are unstable for this time step. On the other hand, the proposed processes are stable and present very good results. There are no appreciable differences between the outcomes of using the MIHOA methods and near exact responses. This is the reason that only one curve is needed to show the fact.

In the second set of analyses, the ability of MIHOA-2U formulation is investigated utilizing a larger time step, $\Delta t = 0.001$ s. In this case, all conditionally stable MIHOA responses make a

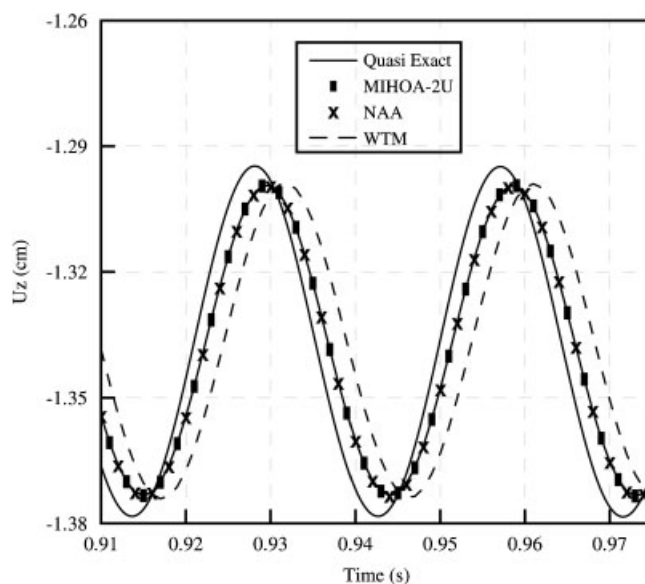


Figure 16. The vertical displacement of the truss peak between 0.91 and 0.975 s.

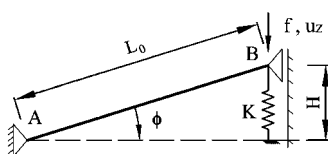


Figure 17. Rod structure.

distance from the true solutions. In order to show the accuracy of the proposed technique, two well-known NAA and WTM algorithms are implemented, as well. Figure 16 displays the vertical displacement curves of the structural peak, between 0.91 and 0.975 s. As it is obvious, the response of the MIHOA-2U and NAA tactics are very near to each other, and also both of these answers are better than the WTM one.

5.5. Rod structure

The undamped SDOF system shown in Figure 17, is excited by the following harmonic vertical load in point B:

$$f(t) = -10 \sin(60t) \text{ N}$$

The values H and $L_0 \cdot \cos \phi$ are 0.02 and 2 m, respectively. The section area of the rod is 6 cm^2 . Moreover, the modulus of elasticity and density of its material are chosen as 21 GPa and 7850 kg/m^3 , correspondingly. The stiffness of spring K is 1 kN/m, as well.

Selecting $\Delta t = 0.015 \text{ s}$, some geometric nonlinear dynamic analyses are performed for the rod structure and the vertical displacement of point B is traced during the first 5 s. The ordinary and the suggested IHOA methods, also the NAA and WTM tactics accomplish this task. For the time between 4.6 and 4.8 s, the outcomes of these analyses along with the quasi-exact solution are plotted in Figure 18. As it is shown in Figure 18, the capability of the conditionally stable schemes of the proposed family is evident, because their responses are close enough to the near exact one. In this case the IHOA-2 and IHOA-3 procedures are unstable. Furthermore, the WTM has also a considerably numerical damping. As it can be seen, IHOA-4 does not lead to good results and NAA reveals large errors, which include both dissipation and dispersion. The MIHOA-2U

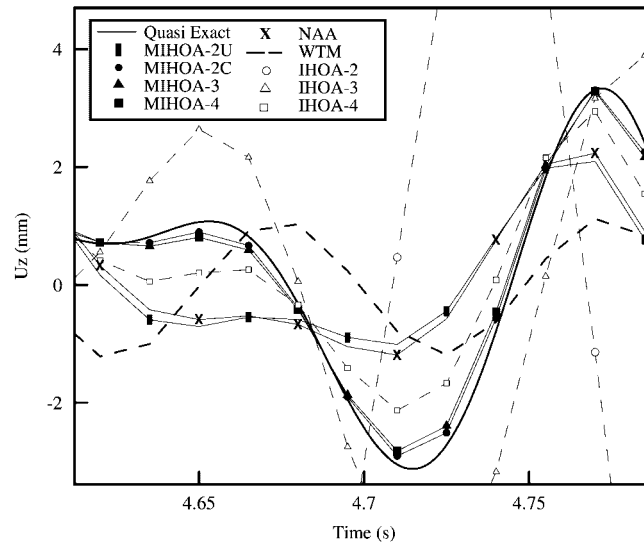


Figure 18. The vertical displacement of point B of rod structure between 4.6 and 4.8 s.

curve is near the NAA one. These two processes show more dissipation and dispersion errors than the MIHOA-2C method.

6. CONCLUDING REMARKS

The three members of recently proposed IHOA time integration family have been considered in this article. The previous study shows that this family presents high accuracy results, when its members are stable [10]. However, its stability conditions are very restrictive. This research is concentrated to cure these weaknesses and suggests a tactic to increase the stability domains of the second-, third- and fourth-order members of the IHOA family. The proposed formulations introduce the parameters β and γ , which was utilized in the Newmark method, in the highest order term of the displacement and velocity extrapolations. In this study, many comprehensive analytical and numerical efforts have been performed to find the optimum values of these two parameters. The outcomes are three new conditionally stable versions, named the MIHOA-2C, 3, and 4 methods. Moreover, an unconditionally stable variant of the IHOA-2 tactic is verified, and denoted MIHOA-2U. All of these algorithms are able to give more stable responses than those belonging to their related members of the IHOA family. Besides, the proposed conditionally stable algorithms show much better results than the Newmark and Wilson- θ methods, and the outcomes of the suggested MIHOA-2U algorithm are near the NAA one. The results of various kinds of benchmark problems verify the capability of the new formulations in both linear and nonlinear dynamic analyses. It is worthwhile to mention that the stability domains of the new conditionally stable processes are wide enough for use in practical problems. From the computational viewpoint since all the MIHOA-2C, 3, and 4 approaches can find near exact solutions in both linear and nonlinear structural analyses, it is more efficient to use the second-order formulation than the third- or fourth-order ones.

NOMENCLATURE

A	amplification matrix
AD	amplitude decay
C	damping matrix
M	mass matrix

m	order of interpolation functions
\mathbf{P}	force vector
PE	period elongation
r	external load
\mathbf{S}	stiffness matrix
T	period of the system
$\mathbf{X}, \dot{\mathbf{X}}, \ddot{\mathbf{X}}$	displacement, velocity, and acceleration vectors
$\Delta t, dt$	time step value
ρ	spectral radius
ξ, η, β, γ	weighted factors
ω	angular frequency
ξ	damping ratio

REFERENCES

1. Razavi SH, Abolmaali A, Ghassemieh M. A weighted residual parabolic acceleration time integration method for problems in structural dynamics. *Journal of Computational Methods in Applied Mathematics* 2007; **7**(3):227–238.
2. Rezaiee Pajand M, Sarafrazi SR. A mixed and multi-step higher order implicit time integration family. *Proceedings of the Institution of Mechanical Engineers, Part C: Journal of Mechanical Engineering Science* 2010; **224**(10):2097–2108.
3. Newmark NM. A method of computation for structural dynamics. *Journal of Engineering Mechanics Division (ASCE)* 1959; **85**(EM3):67–94.
4. Wilson EL, Farhoomand I, Bathe KJ. Nonlinear dynamic analysis of complex structures. *Earthquake Engineering & Structural Dynamics* 1973; **1**:241–252.
5. Wood WL, Bossak M, Zienkiewicz OC. An alpha modification of Newmark's method. *International Journal for Numerical Methods in Engineering* 1981; **15**:1562–1566.
6. Hilber HM, Hughes TJR, Taylor RL. Improved numerical dissipation for time integration algorithms in structural dynamics. *Earthquake Engineering & Structural Dynamics* 1977; **5**:283–292.
7. Chung J, Hulbert GM. A time integration algorithm for structural dynamics with improved numerical dissipation: the generalized- α method. *Journal of Applied Mechanics-Transactions of the ASME* 1993; **60**:371–375.
8. Zhai WM. Two simple fast integration methods for large-scale dynamic problems in engineering. *International Journal for Numerical Methods in Engineering* 1996; **39**(24):4199–4214.
9. Rezaiee Pajand M, Alamatian J. Numerical time integration for dynamic analysis using a new higher order predictor-corrector method. *Engineering Computations* 2008; **25**(6):541–568.
10. Rezaiee Pajand M, Alamatian J. Implicit higher order accuracy method for numerical integration in dynamic analysis. *Journal of Structural Engineering (ASCE)* 2008; **134**(6):973–985.
11. Keierleber CW, Rosson BT. Higher order implicit dynamic time integration method. *Journal of Structural Engineering* 2005; **131**(8):1267–1276.
12. Bathe KJ. *Finite Element Procedures*. Prentice-Hall: New York, 1996.
13. Karimi Rad M, Ghassemieh M. Direct time integration method using second order acceleration for structural dynamic problems. *Proceeding of Fourth National Congress on Civil Engineering*, Tehran, Iran, 2008 (in Persian).
14. Hoff C, Taylor RL. Higher derivative explicit one step methods for nonlinear dynamic problems. Part I: design and theory. *International Journal for Numerical Methods in Engineering* 1990; **29**:275–290.
15. Hoff C, Taylor RL. Higher derivative explicit one step methods for nonlinear dynamic problems. Part II: practical calculations and comparison with other higher order methods. *International Journal for Numerical Methods in Engineering* 1990; **29**:291–301.
16. Gu J, Ma ZD, Hulbert GM. A new load-dependent Ritz vector method for structural dynamics analyses: quasi-static Ritz vectors. *Finite Elements in Analysis and Design* 2000; **36**:261–278.
17. Paz M. *Structural Dynamics: Theory and Computation*. McGraw-Hill: New York, 1979.
18. Anvoner S. *Solution of Problems in Mechanics of Machines I*. Pitman Paperbacks: London, 1970.
19. Sekulovic M, Salatic R, Nefovska M. Dynamic analysis of steel frames with flexible connections. *Computers and Structures* 2002; **80**:935–955.